Section A-Research paper

Effect of Sintering Temperature on PolylactidAcid/Polycaprolactone/Nano-Hydroxyapatite Biocomposites Prepared by The Cold Isostatic Pressing Method

Solechan[1,2*]
[1]Department of Mechanical Engineering, Faculty of Engineering, Diponegoro University, Semarang 50275, Indonesia.
[2]Department of Mechanical Engineering, Universitas Muhammadiyah Semarang, Kampus Kasipah, Semarang 50254, Indonesia.
Agus Suprihanto[1]
[1]Department of Mechanical Engineering, Faculty of Engineering, Diponegoro University, Semarang 50275, Indonesia. Email: agusm90@yahoo.com
Susilo Adi Widyanto[1]
[1]Department of Mechanical Engineering, Faculty of Engineering, Diponegoro University, Semarang 50275, Indonesia.
Joko Triyono[3]
[3]Department of Mechanical Engineering, Sebelas Maret University, Surakarta 57126, Indonesia
Yazid Akbar Mubarok[2]
[2]Department of Mechanical Engineering, Universitas Muhammadiyah Semarang, Kampus Kasipah, Semarang 50254, Indonesia.
Deni Fajar Fitriyana[4]
[4]Department of Mechanical Engineering, Universitas Negeri Semarang, Kampus Sekaran, Gunungpati, Semarang 50229, Indonesia
Januar Parlaungan Siregar[5]
[5]Faculty of Mechanical & Automotive Engineering Technology, Universiti Malaysia Pahang, Pekan 26600, Malaysia
Tezara Cionita[6]
[6]Faculty of Engineering and Quantity Surveying, INTI International University, Nilai 71800, Malaysia
Agustinus Purna Irawan[7]
[7]Faculty of Engineering, Universitas Tarumanagara, Jakarta 11480, Indonesia
***Corresponding Author:** solechan@unimus.ac.id

ABSTRACT

Internal fixation plates are used to heal fractured fractures so they don't get displaced or deformed. Placement of plates to stabilize until the bone heals. The current development of internal fixation plates is made of biocomposite as a substitute for metal materials. PLA/PCL/nHA biocomposite using the cold isostatic pressing method can increase density, decrease porosity and increase bending and tensile strength. One of the main factors affecting the mechanical strength of the internal fixation plate is the sintering temperature. The sintering temperature variations used were 140, 150, and 160^{o}C with the PLA/PCL/nHA biocomposite composition of 80/20/20 %wt. The aim is to obtain an internal fixation plate with the characteristics and mechanical properties of the femur bone. FTIR test results for a mixture of PLA, PCL, and nHA did not form chemical bonds, this is because PLA has hydrophobic properties which makes it difficult for the matrix surface to bond between materials. There are no sharp crystal peaks and broad valleys, so the crystal structure formed is amorphous, indicating that the material is easily degraded. The sintering temperature of 150^{o}C for the PLA/PCL/nHA blends from SEM photos shows a strong interfacial bond, this can increase the density value and decrease the porosity value. These results are consistent with the results of the bending and compressive tests which experienced an increase of 63.1 N and 20.72 N/mm^2.

Keywords : Internal fixation, nano-hydroxyapatite, bone, temperature sintering

1.0 Introduction

Fractures due to traffic accidents are most common in the femur. Fractures can cause bleeding, internal organ injuries, wound infections, and disability [1]. Healing of femoral fractures uses the internal fixation of plates and screws that are placed on cracked or broken parts [2]. The installation is designed to support and support body weight until the bone remodeling or bones heal [3]. Many plates internal fixations are made of metal materials, such as cobalt, stainless steel, titanium, metal alloys, and composites [4,5]. The advantages of metal materials are biological adaptation, biocompatible, corrosion resistance, rigidity, and good mechanical strength [6]. Deficiency can in infection, discomfort, inflammation, traumatic patient, risk of surgical complications, allergic reactions, stress shielding, two surgical operations, and high treatment costs [7-9].

Healing of fractured and broken bones so that they are not displaced or deformed is provided with support in the form of internal fixation plates and screws [1,2]. The installation is designed to stabilize and support the body's weight until the bone heals and reunites [3]. The internal fixation of plates is mostly made of metals such as stainless steel, titanium, and cobalt chrome alloy [4]. Metal materials have high mechanical strength, good biological adaptability, and corrosion resistance [5-7]. However, problems arise due to the installation of the metal plates internal fixation causing infection, allergic reactions, twice the operation process, high handling costs, causing empty parts in the bone, and slowing down the healing process [8-10]. Lacking these materials, biodegradable polymer materials are now more frequently developed [11,12].

Internal fixation plates made of biodegradable materials basically have the ability to be degraded in a biological environment and can be absorbed biologically [13,14]. In addition, it has the advantages of not taking after bone healing, reducing operating costs, traumatic patients, comfort, no holes in the bones, and painless [15-17]. Polylactic Acid (PLA) and Polycaprolactone (PCL) polymer materials are often used in the manufacture of internal fixation plates [18,19]. The choice of this material is due to its gradual degradation properties, biocompatible, non-toxic, ductile, impact toughness, hydrophobic, not physiologically active, hydrophilic, good cell adhesion, and proliferation [15,20]. Solechan et.al (2022) mixed PLA/PCL with varying composition weights using the cold compaction pressure method and sintering at a temperature of 150^{o}C. The result is that the PLA/PCL blends for the 80/20 %wt composition have the best porosity and compressive strength of 8.62% and 51.13 N [21].

Paula and Marcelo (2019) made implants with PLA/PCL blends with a composition of 70/30 %wt using sintering temperature variations of 160, 165 and 170^{o}C at a compaction pressure of 25 MPa. The sintering temperature of 160^{o}C has the best tensile test value of 4.43 MPa [22]. Matta et al. (2014) combined a mixture of PLA/PCL with a composition of 90/10, 80/20, and 70/30. Then sintering at temperatures of 170, 160, 150, 140, and 130^{o}C. The best results are at a composition of 80/20 % wt at a sintering temperature of 150^{o}C with a bending strength of 4.96 MPa and a tensile test of 7.9 MPa [20]. The results of the tensile and compressive strength in this study still cannot match the mechanical strength possessed by the femur [23]. So it is necessary to increase the mechanical strength by adding reinforcing materials to form composite materials [24-27]. Hydroxyapatite (HA) material with a nanometer size is very compatible when combined with PLA/PCL blends [28]. The addition of nano-hydroxyapatite (nHA) to the PCL/PLA blends can increase the mechanical strength and bioactivity of composite materials [19,29-32]. nHA is a ceramic material that is compatible, osteoconductive, non-toxic, non-immunogenic for good absorption, and able to improve mechanical properties [33,34]. Merging of PLA/PCL/HA biocomposite to strengthen

the materials one another to form a material with good mechanical strength [29,35]. Kusumawardani, et.al (2020) made implants with various PLA/PCL/HA biocomposite compositions which were heated at 150^{o}C. Their study showed that the addition of 10 %wt HA is more suitable for bone graft applications [36].

Research conducted by Rezania et al (2022) used PCL/HA material for 3D printer filament which was made at a temperature of 150^{o}C. The best composition, the addition of 20 %wt HA to the mechanical properties showed an increase in compressive strength and young's modulus [37]. Then the research conducted by Sadudeethanakul et al., (2019) using PLA/HA material with a heating temperature of 160^{o}C showed an optimum increase in flexural strength [38]. Jiao, Z, et.al (2019) made a scaffold with an FDM 3D printer. The material is PCL6800 powder added with HA nano and micro. The extruder temperature variable is between 140-170^{o}C for the 3D printer filament manufacturing process. The result is that the addition of nano HA with an extruder temperature of 140 and 150^{o}C has a connected porous structure, uniform particle distribution and increased tensile strength. The tensile strength of nHA is higher than that of micro HA, but the compressive strength is still below that of the manufactured scaffold [26].

The cold isostatic pressing method to form internal fixation plates from PLA/PCL/nHA biocomposites can increase density, reduce porosity, uniform density, reduce distortion, smooth surface, increase tensile, and compressive strength. The factors that influence the cold isostatic pressing method are compaction pressure, sintering temperature, and holding time [39-42]. Therefore, this research analyzes plate fixation of PCL/PLA/nHA biocomposite in 80/20/20 %wt composition with variations in sintering temperature to determine its properties and mechanical properties. Sintering temperature variations ranging from 140-160^{o}C for optimal results have not yet been found. The temperature selection is based on the PLA melting point of 160oC–220^{o}C. It is hoped that the results of this study will be able to obtain an internal plate fixation product with the same properties and mechanical strength as the strength of the femur bone to be implanted to prevent stress shielding.

2.0 MATERIALS & METHODOLOGY

The Specimen in the form of tablets and plates for the testing process. The weight percentage of PLA/PCL/nHA biocomposite composition 80+20/20 %wt. The PLA/PCL blends with a composition weight percentage of 80+20 %wt was mixed then added 20 %wt nHA. The mixing of PLA/PCL/nHA was carried out on a Bexco ball milling machine made in India at 80 rpm for 2 hours. After mixing, the process of making the specimen is placed in the mold. The next process was compacted by cold isostatic pressing at a compacting pressure of 40 MPa at room temperature. The specimen is taken from the mold in the form of a green body which is then sintered. Variations in sintering temperature and parameters for making specimens are shown in Table 1. The sintering process was in a laboratory oven type D1570 made in Taiwan with a holding time of 2 hours. Specimens are cleaned and prepared according to the test standards of each test process. Internal fixation plates specimen testing starts with Fourier Transform Infrared Spectroscopy (FTIR), Scanning Electron Microscope (SEM), density, porosity, bending, and tensile tests.

Tabel 1. Parameters of the PLA/PCL/nHA biocomposite and sintering temperature

Composition PLA/PCL/nHA (%wt)	Compaction Pressure (Mpa)	Temperature (^{o}C)	Specimen Testing
80/20/20	40	140 150	Testing SpesFTIR, XRD, SEM, density, porosity, bending & tensile

tests

PLA/PCL/nHA materials are imported from several countries. PLA polymer in powder form with chemical formula $(C_6H_8O_5)n$, density 1.24 gr/cc, melting point 160-220℃ was made by Repreper Tech Co, Kowloon, Hong Kong. The PCL material was obtained from Solve Interox Limited Warrington UK, in powder form with the chemical formula $(C_6H_8O_2)x$, density 1.1 gr/cc and melting point 58-60℃.

For other materials, it is nano-Hydroxyapatite (nHA) powder with >99% purity and grain size of 500-100 nm. White nHA powder with a HA density of 3.076 gr/cm^3 and a melting point of 1100℃. nHA is produced by Graphene Composite Kft, Kapsorvar Hungary.

3.0 Results and Discussion

3.1. Fourier Transform Infrared Spectroscopy

The FTIR spectrum graph of the PLA/PCL/nHA biocomposite is shown in Figure 1. The peak chemical bonds of PLA/PCL/nHA are located at 2921.67 cm^{-1} and 2853.89 cm^{-1}. Spectrum graphs were analyzed using the IR Absorption characteristics table and compared with the spectra of PLA, PCL and pure nHA. The spectrum measurement range is from 4000 to 500 cm^{-1}. The material spectrum area corresponds to the table of absorption characteristics, elements belonging to PLA ($C_6H_8HA_{I5}$) and PCL ($C_6H_{10}HA_{I2}$) are in the results of the FTIR spectra of elements C, H, and O [42]. The spectrum graph shows the wideband for C–H Stitch owned by PCL at the peak of 2921.67 cm^{-1}. It also indicates that the peak is in the stretching band region according to pure PCL studies which is detected as CH_2 [43]. For the spectrum of PLA which has a C=O stretch bond which shows a strain band detected at the peak of the spectrum 1714.50 cm^{-1}. This corresponds to the stretch C=O bond that belongs to the group of carboxylic acids [44]. PLA is inert so it does not have a group chain with a reactive side [45]. In the observation there were also C-O stretching ester bonds at a frequency of 1320-1000 cm^{-1} which were detected at the peak of 1155.65 cm^{-1}. These results represent the spectrum of the PLA/PCL blends formed [21,44,46].

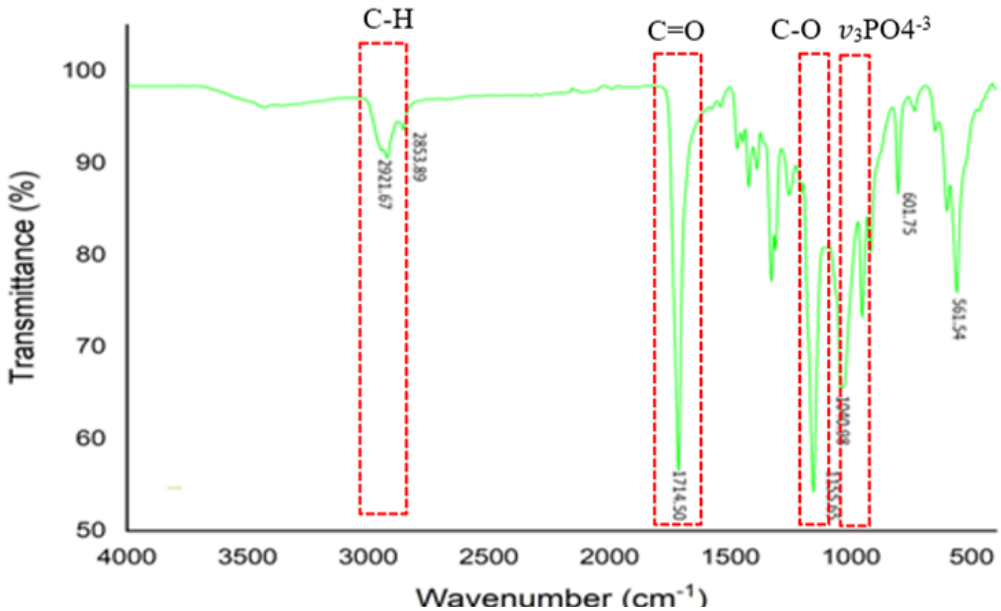

Figure 1. FTIR spectrum on PLA/PCL/nHA composite materials

The nHA material with a phosphate (v_3PO4^{-3}) absorption band can be identified with a maximum of around 1030 cm^{-1} and a shoulder of around 1090 cm^{-1} [47]. In his analysis for the crystallinity spectrum of phosphate can evaluate the absorption of phosphate v_3PO4^{-3}. Calcium phosphate can be characterized by the presence of an absorption band v_4 in the form of a maximal split in the presence of bands at 564 cm^{-1} and 602 cm^{-1}. The results showed that the identified band was around 1040.98 cm^{-1}. The results of this study can be concluded that the mixture of PLA, PCL, and nHA materials does not form chemical bonds, because PLA has hydrophobic properties [48]. Some findings of biocomposite materials on the PLA surface cannot chemically bond with the nHA powder surface [49].

3.2. X-Ray Diffraction

XRD testing on PLA/PCL/nHA biocomposite to observe the crystal form and structure contained in the specimen. Figure 2 shows the peaks of the PLA/PCL/nHA bicomposite with three degrees of crystallinity detected. Three specimens at sintering temperatures of 140, 150, and 160°C had peaks of 2θ= 22.77°, 2θ= 24.07°, and 2θ= 22.51°. The three peaks formed from the peaks of the PLA/PCL/nHA biocomposite with different sintering temperature variations according to a study conducted by Hooshmand, et.al (2014) [50]. The PLA/PCL/nHA biocomposite shows wide peaks positioned between 10° to 40° and shows prominent peaks at 22° to 24°. The absence of sharp crystalline peaks and broad bases in the PLA/PCL/nHA biocomposite indicates that the crystal structure formed is amorphous. This is in accordance with the study of Hou, et.al (2019) that the XRD pattern of a mixture of PLA, PCL and nHA with overlapping PCL crystal peaks in amorphous PLA [51]. This is characterized by indistinct peaks with low absorption intensity [52]. The process of manufacture specimens with different melting points between materials causes the formation of amorphous crystal structures. A low level of crystallity indicates that the material is easily degraded in the body [51,53].

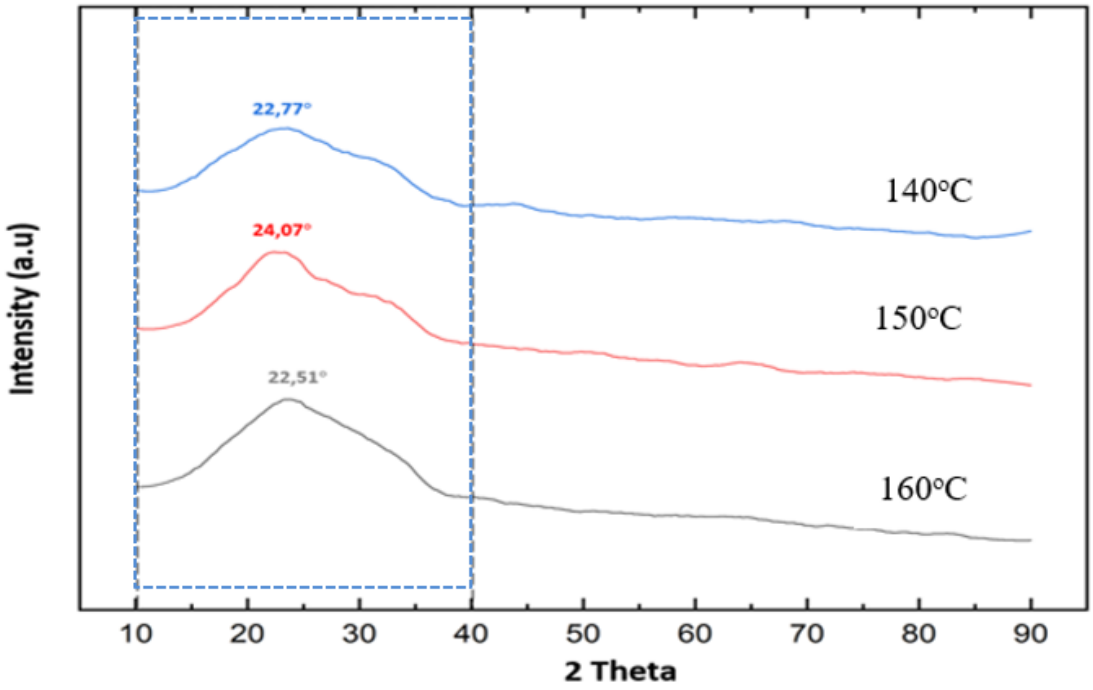

Figure 2. XRD diffraction graph of PLA/PCL/nHA composite material

Although PLA and PCL have semi-crystalline properties after being mixed they become amorphous in the PLA/PCL blends [54]. Amorphous properties are characterized by sharp peaks with low absorption

intensity. This is due to the different degrees of deformation in the PLA, PCL and nHA molecules [21]. Polymers with different degrees of molecular deformation and high molecular weight are the main factors that determine the degree of crystallinity [55].

PLA/PCL/nHA biocomposite has a low level of crystallinity which can shorten the degradation time [49,56]. The intensity of the diffraction peaks of the PLA/PCL/nHA biocomposite does not increase with increasing sintering temperature, because the formation of crystal structures is influenced by molecular weight [51]. nHA causes a less uniform structure, irregular crystallization, and increased spacing between layers. The presence of a low crystalline phase in all bicomposite specimens indicates an inhibition of crystallization in the polymer matrix [57,58].

3.3. Scanning Electron Microscope (SEM)

The results of the SEM photos on a tablet specimen of PLA/PCL/nHA biocomposite obtained the morphological structure of the specimen surface which was influenced by the sintering temperature variable shown in Figure 3. SEM photo with 5000x magnification shows the morphological structure of the nHA powder clearly visible in the form of white cubes. The PLA with the highest composition weight is in the form of black lumps and is evenly distributed throughout the surface. Meanwhile, the PCL is in the form of white lumps mixed with PLA. The results of SEM photos of PLA/PCL/nHA biocomposites are in accordance with research conducted by Ferri, et.al (2016) and Wachirahuttapong, et.al (2016) [23,59]. The SEM photo of the specimen at a temperature of 140^{o}C in Figure 3a shows that the PLA/PCL/nHA biocomposite still does not look perfectly bonded to each other because the PLA has not melted. PLA and PCL are separate and have no ties to one another. PCL and nHA are positioned above the PLA surface and are only attached as a small amount between the materials so that the bond between the surfaces is not too strong. This is because PLA is in the form of a semi-crystal with a slow crystallization rate, is hydrophobic, and if it has not reached the melting point it will be difficult to mix with other materials [60]. Very high porosity and very deep holes all over the specimen surface due to too low sintering temperature [29].

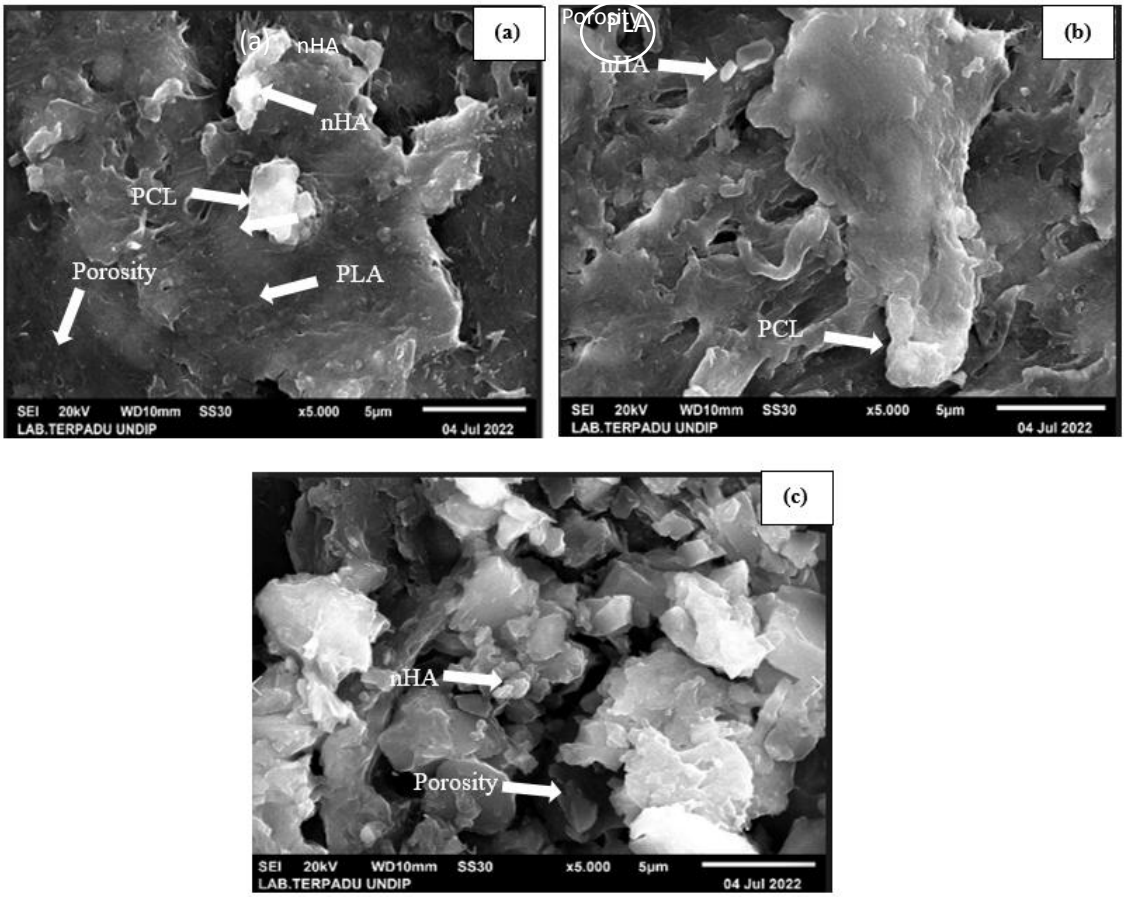

Figure 3. SEM photo of PLA/PCL/nHA biocomposite a). 140^{o}C, b). 150^{o}C, c). 160^{o}C

Figure 3a SEM photo of a specimen with a temperature of 150^{o}C shows changes in the PLA/PCL/nHA blends which binds each other between the material and the mixture evenly throughout the specimen surface which can reduce the porosity value. The sintering temperature of 150^{o}C for PLA material has entered the semi-liquid phase, causing the surface energy and interface contact between the materials to increase and reduce the agglomeration of nHA particles [61-63].

The porosity value is lower, the pores are small, and only a small portion of nHA powder is not mixed with the PLA/PCL blends. This sintering temperature also accelerates diffusion to form stronger interfacial bonds [41,64]. Increasing the sintering temperature to 160^{o}C for a mixture of materials that do not bond well with each other and the nHA powder has a lot of loose bonds as shown in Figure 3c. This is because the PLA material has entered the melting point phase, which is between 150–162^{o}C [29]. The surface of the specimen forms an empty space due to air bubbles due to the boiling of the PLA liquid. These results are in line with Noroozi's research. N, et.al (2020) high a sintering temperature causes the cavities to enlarge and most of the bonds between materials release which occur at the ends and branches of the mixture [65]. how to get optimal results, preferably the sintering temperature is 70-90% below the melting point of the matrix material [66].

3.4. Density dan Porosity

The high or low porosity value depends on the density value [67]. The PLA/PCL/nHA biocomposite with various sintering temperatures for the density and porosity test results is shown in Figure 4. The sintering temperature of 140^{o}C has the lowest density of 1.23 g/cm^{3} and the highest porosity with a value of 5.75%.

The low density results from enlarged pores and deeper porosity cavities which is proven from SEM photos. The high porosity is caused by the mixture of PLA, PCL, and nHA there is no bond between the material surfaces because the matrix material is under the solid phase. In the solid phase, the PLA/PCL blends has not yet fused and nHA cannot be bound and covered by the matrix. The sintering temperature is 140ºC for low viscosity, as a result, the ability to flow to fill a small space causes the density to decrease [68,69]. The sintering temperature was increased to 150°C for the density value increased by 3.14% (1.27 g/cm^3) and the porosity decreased by 18.26%. The increase in the density value and decrease in the porosity value is due to the wider surface contact area between the materials and changes in the structure of the particles which can reduce the pore cavities [70].

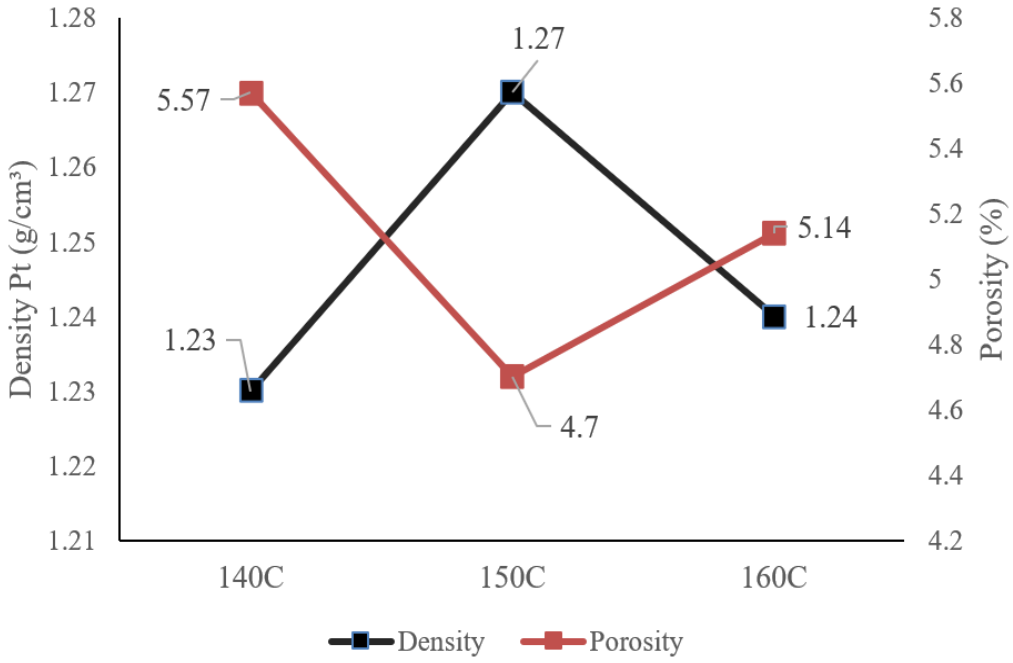

Figure 4. Density and porosity test results on composite materials

The bond between materials is stronger because the matrix material has experienced a liquid or melting phase, thereby accelerating the diffusion process in the sintering process [21].

The melting temperature of the matrix material for PLA is between 152-220℃ and for PCL between 58-60℃ [29,61,71]. The results of the density and porosity values at the sintering temperature of 160°C for the values change. Density decreased by 2.36% (1.24 g/cm^3) and porosity increased by 8.56%. The increase in the porosity value is indicated by enlarged pores due to the matrix phase being in the liquid or boiling phase which results in the formation of air bubbles. This incident causes air to be trapped in the PLA/PCL blends and the matrix bond with nHA is released [52,72]. Decreasing and increasing the sintering temperature at 140 and 160°C increases the porosity and decreases the density. The most optimal sintering temperature is 150°C because the PLA/PCL/nHA biocomposites can be mixed, the pores are reduced and the matrix material's melting point is below the melting point of 70-90% Tm [66,73].

3.5. Bending Test

The graph of bending test results for several specimens of PLA/PCL/nHA biocomposite with variations in sintering temperature is shown in Figure 5. The results for bending strength are in newtons (N) and displacement in millimeters (mm). Bending test results at a sintering temperature of 140°C for a bending

strength of 45.50 N with a displacement of 5.65 mm. This compressive strength and displacement is the lowest compared to other specimens. The bond strength of the material interface and the resulting flexural strength decrease due to the sintering temperature being too low [74]. The low sintering temperature is unable to reach the semi-liquid phase of the matrix material, this causes the pores to become large and the density to decrease. These results are in accordance with research conducted by Haq, R. et.al., (2019) [75].

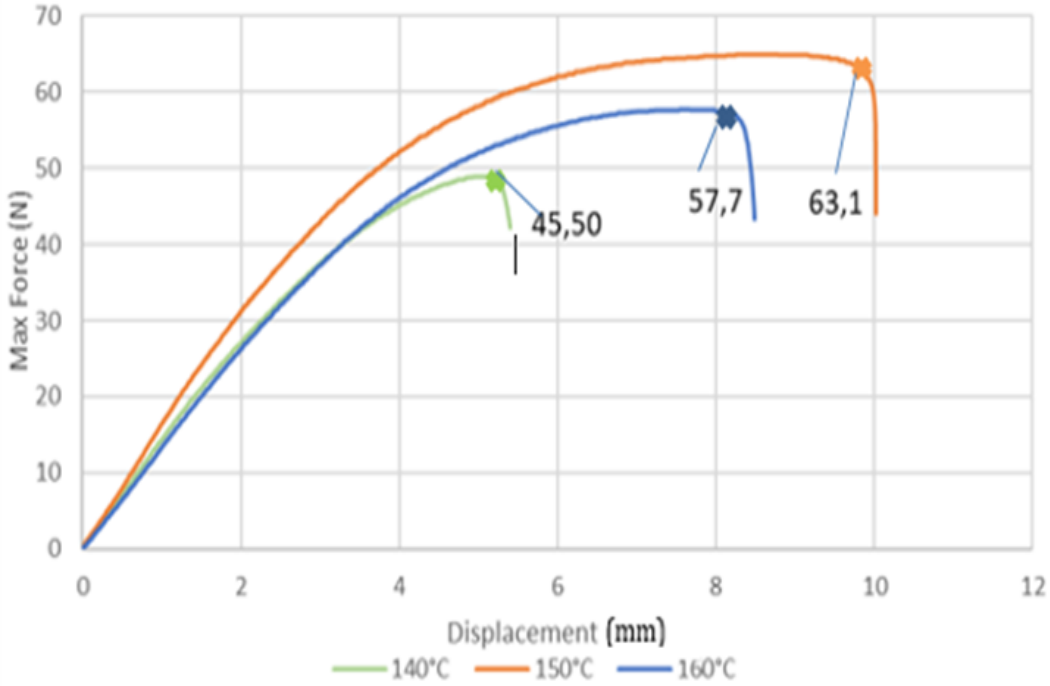

Figure 5. Bending test results for PLA/PCL/nHA composite materials

The sintering temperature was increased to 150oC for the bending strength increased by 27.9% (63.1 N) with a displacement of 9.8 mm (24.3% increase). The increase in compressive strength and displacement is very significant. This increase was due to the mixture of PLA, PCL, and nHA being able to mix well with the strong interfacial bonds shown by the SEM photos. The sintering temperature of 150^{o}C makes the matrix material experience a liquid phase which makes the material interface bonds bond and accelerates the diffusion process.

This results in an increase in bending strength caused by a decrease in the porosity value and an increase in the density value. The increase in bending strength is also affected by the increase in the dispersion of nHA particles that can cover the pores [69,76].

An increase in the centering temperature of 160^{o}C did not increase the bending strength and displacement but decreased. Bending strength decreased by 8.6 % (57.7 N) with a displacement of 8.2 mm (decreased 16.3%). This corresponds to the decreased density value and increased porosity [38]. The results of the SEM photos show that the bond between the materials is weak with the bond between the materials being released, besides that the powder contact area is wider due to the sintering temperature being too high. The matrix material experiences a liquid phase causing air bubbles to form resulting in air being trapped in the specimen. The air trapped in the specimen is unable to escape because the holding time is too fast, causing larger pores [77,78]. The presence of nHA in a matrix with a high sintering temperature results in agglomeration as an initial fracture propagation due to the stress concentration during the bending test

[69,79]. Bending strength is highest at sintering temperature of 150^{o}C for bending strength still below the femur of 130 N/mm^2 [80].

3.6. Tensile Test

Based on the results of the tensile test graph on the PLA/PCL/nHA biocomposite with variations in sintering temperature for the lowest tensile strength and elongation, the specimen was 140^{o}C, as shown in Figure 6. This sintering temperature has a tensile strength of 17.18 N/mm^2 and 3.2% elongation. The low tensile strength is caused by the PLA/PCL matrix being unable to bind and envelop nHA. The temperature is too low to make the matrix has not experienced a semi-liquid phase. The matrix material has not yet melted so that the bond between the material surfaces becomes weak, thereby reducing the tensile and compressive strength [18,23,81]. The bond strength between materials is only obtained from high compaction pressure which can increase density but still high porosity. The sintering temperature was increased to 150oC for an increase in tensile strength of 17.1% (20.72 N/mm^2) and elongation to 4.6%. The increased tensile strength is evidenced from SEM photos which show lower porosity, smaller pores and increased density. The sintering temperature of 150^{o}C is in the range of 70-90% below the melting point of the matrix material and is in a semi-liquid state to support the diffusion process between materials [63,82]. The condition of the semi-liquid phase makes the bond between the matrix (PLA/PCL) and nHA stronger, the contact area is larger, the flow is good, the agglomerate is reduced and the pores are smaller [83,84].

The sintering temperature of 160^{o}C, the density value decreases and the porosity increases, making the tensile strength slightly weaker. The tensile strength obtained is 20.01 N/mm^2 and the elongation is 4.4%. The weakening of the tensile strength is caused by the release of bonds between the materials and the emergence of large new pores due to too high sintering temperature. The sintering temperature of 160^{o}C for the matrix condition is already in the boiling phase and generates a lot of air bubbles [60,85]. The large number of air bubbles in the specimen causes porosity, although not as much as the sintering temperature of 140^{o}C. The tensile test results of the three specimens for elongation values were still low, namely below 5%. This shows that the PLA/PCL/nHA biocomposite is brittle, brittle, easily broken and inelastic [67,86]. This is due to the too large percentage of the nHA composition which makes it brittle and high in stiffness [87]. The best results of the tensile test were at a sintering temperature of 150^{o}C, but the tensile strength was still far below the tensile strength of the femur of 50 MPa, so it was necessary to find the right sintering temperature [11].

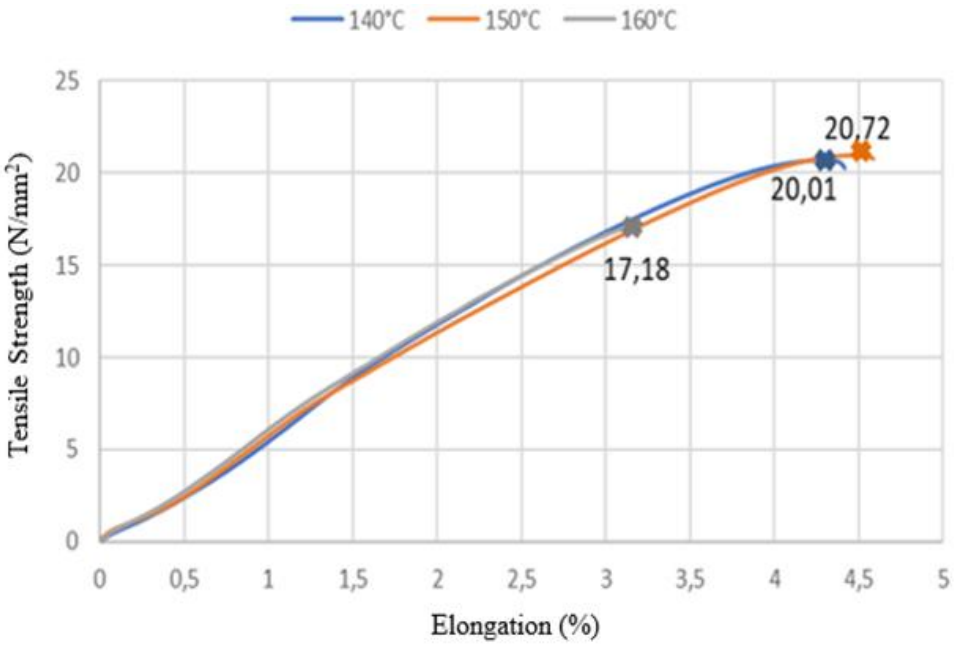

Figure 6. Tensile test results for PLA/PCL/nHA composite materials

4.0 Conclusions

The PLA/PCL/nHA biocomposite from the FTIR spectra chart detected C–H and CH_2 elements belonging to PCL, C=O bonds and C-O ester bonds detected belonged to PLA, and the absorption band v_3PO4^{-3} was detected to belong to nHA. The mixture of PLA, PCL, and nHA materials does not form chemical bonds because PLA has hydrophobic properties. The PLA/PCL/nHA biocomposite showed non-sharp peaks and wide valleys indicating that the crystal structure formed was amorphous. The amorphous crystal structure has a low level of crystallity and indicates that the material is easily degraded. Sintering temperature of 150^{o}C from SEM photos shows a mixture of PLA/PCL/nHA that binds to each other at the material interface, the mixture is uniform, and the pores are smaller. This results in an increase in the density value and a decrease in the porosity value due to the wider surface contact area between the materials. The results of bending and compressive tests at sintering temperatures of 150^{o}C had the highest values of 63.1 N and 20.72 N/mm^2. This result is still far below the mechanical strength of the femur used as an implant medium, so it is necessary to find the optimal sintering temperature.

Acknowledgements

The author would like to thanks Engeenering Faculty Universitas Muhammadiyah Semarang Indonesia, which has provided funding for Research disertation of fiscal year 2022-2023. The material characterization partially supported by research fund from Department Mechanical Engineering, Faculty of Engineering, Diponegoro University, 2023.

References

1. Helmi, Zairin Noor. 2012. Buku Saku Kedaruratan di Bidang Bedah Ortopedi. Jakarta: Salemba Medika. ISBN 978-602-7670-18-1

2. Wongchai, B. (2012). The effect of the configuration of the screw fixation on the interfragmentary strain. American Journal of Applied Sciences, 9(6), 842–845. https://doi.org/10.3844/ajassp.2012.842.845

3. Latif, M. N., Nabawi, R. A., Nanda, I. P., & Sahputra, R. E. (2019). Simulasi Dan Analisis Locking Compression Plate Implan Tulang Paha Menggunakan Metoda Finite Element Analysis. Jurnal Sains dan Teknologi, 19(1), 72–78.

4. Saidpour, S. H. (2006). Assessment of Carbon Fibre Composite Fracture Fixation Plate Using Finite Element Analysis. Annals of Biomedical Engineering, 34(7), 1157–1163. doi:10.1007/s10439-006-9102-z.

5. Juutilainen T, Pätiälä H, Ruuskanen M, Rokkanen P. 2017, Comparison of costs in ankle fractures treated with absorbable or metallic fixation devices. Arch Orthop Trauma Surg1997;116:204-8..

6. Böstman O., Pihlajamäki H., 1996, Routine implant removal after fracture surgery: a potentially reducible consumer of hospital resources in trauma units. J Trauma;41:846-9.

7. Ritonga, I. (2020). Karakteristik Implant Failure Pada Pasien Yang Menjalani Orif Plate And Screw Pada Anggota Gerak Bawah Di RSUP Ham Medan Tahun 2015-2019. Universitas Sumatera Utara Medan.

8. Alisdair R.. Mac Leod., Pankaj Pankaj., Hamish A., Simpson R.W., 2012, Does screw-bone interface modeling matter in finite element analyses, Journal of Biomechanics, vol. 45, pp. 1712-1716.

9. Rusrial, Gunawarman, & Affa, J. (2014). Pengaruh Ukuran serta Sudut Pemasangan Pin terhadap Kekuatan Sambungan Tulang Pasca Fraktur. 21(1), 55–59.

10. Triyono. J., 2015, Terinspirasi Kelainan Tulang, Suara Merdeka Cetak, www.berita.suaramerdeka.com, diakses pada tanggal Kamis , 2 April 2015.

11. Corcione, C.E., F. Gervaso., F. Scalera., F. Montagna., T. Maiullaro., A. Sannino., A. Maffezzoli., 2017, 3D printing of hydroxyapatite polymer-based composites for bone tissue engineering, J. Polym. Eng 741.

12. Toro C, Robiony M, Zerman N, Politi M., 2005, Resorbable plates in maxillary fixation. A 5year experience. Minerva Stomatol;54(4):199-206.

13. Estes, A. R., & Oladeji, L. O. (2015). Arthroscopic treatment of tibial spine malunion with resorbable screws. American Journal of Orthopedics (Belle Mead, N.J.), 44(5), E160–E164.

14. Vatchha, S. P., Kohli, A., Tripathi, S. K., & Nanda, S. N. (2015). Biodegradable Implants in Orthopaedics. Annals Of International Medical and Dental Reseach, 1(1), 3–8.

15. Neut, D., Kluin, O. S., Crielaard, B. J., Van Der Mei, H. C., Busscher, H. J., & Grijpma, D. W. (2009). A biodegradable antibiotic delivery system based on poly-(trimethylene carbonate) for the treatment of osteomyelitis. Acta Orthopaedica, 80(5), 514–519. https://doi.org/10.3109/17453670903350040

16. Singh, S. K. (2016). Understanding the effect of extrusion processing parameters on physical, nutritional and rheological properties of soy white flakes based aquafeed in a single screw extruder. Thesis and Dissertations, Paper 956.

17. Mochane, M. J., Motsoeneng, T. S., Sadiku, E. R., Mokhena, T. C., & Sefadi, J. S. (2019). Morphology and properties of electrospun PCL and its composites for medical applications: A mini review. Applied Sciences (Switzerland), 9(11), 1–17. https://doi.org/10.3390/app9112205

18. T. Xu, Q., Yao, J.M. Miszuk., H.J. Sanyour., Z. Hong., H. Sun., H. Fong., 2018, Tailoring weight ratio of PCL/PLA in electrospun three-dimensional nanofibrous scaffolds and the effect on osteogenic differentiation of stem cells, Colloids and Surfaces B: Biointerfaces. Volume 171, 1 November 2018, Pages 31-39

19. Pietrzykowska, E., Romelczyk-Baishya, B., Wojnarowicz, J., Sokolova, M., Szlazak, K., Swieszkowski, W.,Lojkowski, W., 2020, Preparation of a Ceramic Matrix Composite Made of Hydroxyapatite Nanoparticles and Polylactic Acid by Consolidation of Composite Granules. Nanomaterials, 10(6), 1060. doi:10.3390/nano10061060..

20. Matta, A. K., Rao, R. U., Suman, K. N. S., & Rambabu, V. (2014). Preparation and Characterization of Biodegradable PLA / PCL Polymeric Blends. Procedia Materials Science, 6(Icmpc), 1266–1270. https://doi.org/10.1016/j.mspro.2014.07.201.

21. Solechan, Suprihanto, A., Widyanto, S. A., Triyono, J., Fitriyana, D. F., Siregar, J. P., & Cionita, T. (2022). Investigating the Effect of PCL Concentrations on the Characterization of PLA Polymeric Blends for Biomaterial Applications. Materials, 15. https://doi.org/https:// doi.org/10.3390/ma15207396 Academic

22. Paula do Patrocínio Dias and Marcelo Aparecido Chinelatto., 2019, Effect of Poly(ε-caprolactone-b-tetrahydrofuran) Triblock Copolymer Concentration on Morphological, Thermal and Mechanical Properties of Immiscible PLA/PCL Blends, Tech Science Press, DOI: 10.32604/jrm.2019.00037, JRM, 2019, vol.7, no.2, www.techscience.com.

23. Ferri, J., M., Fenollar., O., Jorda-Vilaplana, A., García-Sanoguera, D., & Balart, R., 2016, Effect of miscibility on mechanical and thermal properties of poly(lactic acid)/ polycaprolactone blends. Polymer International, 65(4), 453–463. doi:10.1002/pi.5079.

24. Xibao Chen., Chunxia Gao., Jiawei Jiang., Yaping Wu., Peizhi Zhu., Gang Chen., 2019, 3D printed porous PLA/nHA composite scaffolds with enhanced osteogenesis and osteoconductivity in vivo for bone regeneration, Biomedical Materials, IOP Publishing, BMM-102954.R1

25. Solechan., Rubijanto, J., Triyono, J., & Pujiyanto, E., 2019, Study of Making Implant Plate and Screen of Femur Bone Internal Fictation From Hydroxyapatit Bovine And Polymer Biodegradation Material Using 3D Printers On Mechanical Strength. IOP Conference Series: Materials Science and Engineering, 494, 012070. doi:10.1088/1757-899x/494/1/012070.

26. Jiao, Z., Luo, B., Xiang, S., Ma, H., Yu, Y., & Yang, W., 2019., 3D printing of HA / PCL composite tissue engineering scaffolds. Advanced Industrial and Engineering Polymer Research. doi:10.1016/j.aiepr.2019.09.003.

27. Jun Wei Lil., et.al,. 2019, Application of Biodegradable Materials in Orthopedics, Journal of Medical and Biological Engineering https://doi.org/10.1007/s40846-019-00469-8, Taiwanese Society of Biomedical Engineering 2019

28. Xiao, X., Liu, R., & Huang, Q. (2008). Preparation and characterization of nano-hydroxyapatite/polymer composite scaffolds. Journal of Materials Science: Materials in Medicine, 19(11), 3429–3435. https://doi.org/10.1007/s10856-008-3499-x.

29. Alizadeh-osgouei, M., Li, Y., & Wen, C. (2019). A comprehensive review of biodegradable synthetic polymer-ceramic composites and their manufacture for biomedical applications. Bioactive Materials, 4(1), 22–36. https://doi.org/10.1016/j.bioactmat.2018.11.003.

30. Karageorgiou, V., & Ã, D. K. (2005). Porosity of 3D biomaterial scaffolds and osteogenesis. 26, 5474–5491. https://doi.org/10.1016/j.biomaterials.2005.02.002

31. Zein, I., Hutmacher, D. W., Tan, K. C., & Teoh, S. H. (2002). Fused deposition modeling of novel scaffold architectures for tissue engineering applications. Biomaterials, 23(4), 1169–1185. doi:10.1016/s0142-9612(01)00232-0.

32. Termal, S., Pcl, K., & Peg, P. L. A. (2021). Karakterisasi, Sifat Termal dan Biologis Komposit PCL/PLA/PEG/N-HA. 11, 9017–9026..

33. Armentano, I., Dottori, M., Fortunati, E., Mattioli, S., & Kenny, J. M. (2010). Biodegradable polymer matrix nanocomposites for tissue engineering: A review. Polymer Degradation and Stability, 95(11), 2126–2146. https://doi.org/10.1016/j.polymdegradstab.2010.06.007

34. Ramos, D. M., Dhandapani, R., Subramanian, A., Sethuraman, S., & Kumbar, S. G., 2019, Clinical complications of biodegradable screws for ligament injuries. Materials Science and Engineering: C, 110423. doi:10.1016/j.msec.2019.110423.

35. Saifudin Alie Anwar., Solechan., 2015, studi pembuatan filamen komposit FDM untuk print 3D dari material Hidoryapatite bovine dan polimer PCL untuk scaffolds mandibular, Jurnal Gardan, vol 2 edisi 1, hal 6-12.

36. Kusumawardani, C. D. N., Chondro, R. T., Andrian, I., & Sari, R. P. (2020). Pengaruh penambahan hidroksiapatit terhadap porositas dan compressive strength basis resin akrilik heat-cured, Effect of hydroxyapatite addition towards porosity level and compressive strength of heat-cured acrylic resin base. Jurnal Kedokteran Gigi Universitas Padjadjaran, 32(2), 91. https://doi.org/10.24198/jkg.v32i2.26627.

37. Rezania, N., Asadi-eydivand, M., Abolfathi, N., Bonakdar, S., & Solati-hashjin, M. (2022). Three-dimensional printing of polycaprolactone / hydroxyapatite bone tissue engineering scaffolds mechanical properties and biological behavior. Journal of Materials Science: Materials in Medicine (2022) 33:31. https://doi.org/10.1007/s10856-022-06653-8

38. Sadudeethanakul, S., Wattanutchariya, W., Nakkiew, W., Chaijaruwanich, A., & Pitjamit, S. (2019). Bending strength and Biological properties of PLA- HA composites for femoral canine bone fixation plate. IOP Conference Series: Materials Science and Engineering. https://doi.org/10.1088/1757-899X/635/1/012004.

39. Morris, K.J. 1991, Cold Isostatic Pressing. In Concise Encyclopedia of Advanced Ceramic Materials; BROOK, R.J.B.T.-C.E. of A.C.M., Ed.; Pergamon: Oxford, 1991; pp. 84–88 ISBN 978-0-08-034720-2.

40. German RM, Bose A., 1997, Injection Molding of Metals and Ceramics: Metal Powder Industries Federation. ISBN 187895461X, 9781878954619

41. Arifin, A., Sulong, A. B., Muhamad, N., Syarif, J., & Ramli, M. I. 2014, Material processing of hydroxyapatite and titanium alloy (HA/Ti) composite as implant materials using powder metallurgy: A review. Materials & Design, 55, 165–175. doi:10.1016/j.matdes..09.045

42. Solechan, Prasetyo, M. T., Triyono, J., & Pujiyanto, E. (2021). Pengujian Sifat Mekanik Implan Plate dan Sekrup Fiksasi Internal Tulang Femur Dari Material Hidroksiapatit Bovine Dan Polimer Biodegradasi Menggunakan Printer 3D. TRAKSI: Majalah Ilmiah Teknik Mesin, 20(1), 45–58. https://doi.org/https://dx.doi.org/10.26714/traksi.21.1.2021.27-37

43. Shojaei, S., Nikuei, M., Goodarzi, V., Hakani, M., Khonakdar, H. A., & Saeb, M. R. (2019). Disclosing the role of surface and bulk erosion on the viscoelastic behavior of biodegradable poly(ε-caprolactone)/poly(lactic acid)/hydroxyapatite nanocomposites. Journal of Applied Polymer Science, 136(10). https://doi.org/10.1002/app.47151

44. Prajongtat, P., Sriprachuabwong, C., Wongkanya, R., & Dechtrirat, D. (2019). Moisture-Resistant Electrospun Polymer Membranes for Efficient and Stable Fully Printable Perovskite Solar Cells Prepared in Humid Air Moisture-Resistant Electrospun Polymer Membranes for E ffi cient and Stable Fully Printable Perovskite Solar Cells Prepa. August. https://doi.org/10.1021/acsami.9b05032

45. Rasal, R. M., Janorkar, A. V, & Hirt, D. E. (2010). Progress in Polymer Science Poly (lactic acid) modifications. Progress in Polymer Science, 35(3), 338–356. https://doi.org/10.1016/j.progpolymsci.2009.12.003

46. Singla, P., Mehta, R., Berek, D., & Upadhyay, S. N. (2012). Microwave Assisted Synthesis of Poly (Lactic acid) and its Characterization using Journal of Macromolecular Science , Part A : Pure and Applied Chemistry Microwave Assisted Synthesis of Poly (lactic acid) and its Characterization using Size Exclusion. Journal of Macromolecular Science, Part A: Pure and Applied Chemistry, 49(11), 963–970. https://doi.org/10.1080/10601325.2012.722858

47. Dahlan, K., Sari, Y. W., Yuniarti, E., & Soejoko, D. S. (2006). Karakterisasi Gugus Fosfat dan Karbonat dalam Tulang Tikus dengan Fourier Transform Infrared (FT-IR) Spectroscopy. Indonesian Journal of Materials Science, 221–224.

48. Warastuti, Y., Abbas, B., & Suryani, N. (2017). Pembuatan Komposit Polikaprolakton-Kitosan-Hidroksiapatit Iradiasi Untuk Aplikasi Biomaterial. Metalurgi, 28(2), 149–160. http://ejurnalmaterialmetalurgi.com/index.php/metalurgi/article/view/256

49. Lu, Y., Chen, Y., & Zhang, P. (2016). Preparation and Characterisation of Polylactic Acid (PLA)/ Polycaprolactone (PCL) Composite Microfibre Membranes. FIBRES & TEXTILES in Eastern Europe, 24(117), 17–25. https://doi.org/10.5604/12303666.1196607

50. Hooshmand, T., Abrishamchian, A., Najafi, F., Mohammadi, M., Najafi, H., & Tahriri, M. (2014). Development of sol-gel-derived multi-wall carbon nanotube / hydroxyapatite nanocomposite powders for bone substitution. Journal of Composite Materials 0(0), 1–7. https://doi.org/10.1177/0021998313475368

51. Hou, A.-L., & Qu, J.-P. (2019). Super-Toughened Poly(lactic Acid) with Poly(ε-caprolactone) and Ethylene-Methyl Acrylate-Glycidyl Methacrylate by Reactive Melt Blending Ao-Lin. Polymers.

52. Åkerlund, E.; Diez-escudero, A.; Grzeszczak, A. The Effect of PCL Addition on 3D-Printable PLA / HA Composite Filaments for the Treatment of Bone Defects. Polymers (Basel). 2022, 14, 1–17.

53. Albertsson, A.-C. (2002). Degradable Aliphatic Polyesters (Polymer, volume 157). Springer. Part of the book series, ISBN: 978-3-540-45734-3

54. Boland ED, Pawlowski KJ and Barnes CP et al, 2006, Electrospinning of bioresorbable polymer for tissue engineering scaffolds[M]. USA Washington: AMER CHEMICAL SOC, 918: 188-204

55. Haroosh HJ, Chaudhary DS and Dong Y, 2012, Electrospun PLA/PCL fibers with tubular microclay: Morphological and structural analysis [J]. Journal of Applied Polymer Science; 124(5): 3930-3939.

56. Silverajah, V.S.G.; Ibrahim, N.A.; Yunus, W.M.Z.W.; Hassan, H.A.; Woei, C.B. A Comparative Study on the Mechanical, Thermal and Morphological Characterization of Poly(Lactic Acid)/Epoxidized Palm Oil Blend. Int. J. Mol. Sci. 2012, 13, 5878–5898.

57. Jing, X.; Mi, H.-Y.; Turng, L.-S. Comparison between PCL/Hydroxyapatite (HA) and PCL/Halloysite Nanotube (HNT) Composite Scaffolds Prepared by Co-Extrusion and Gas Foaming. Mater. Sci. Eng. C 2017, 72, 53–61, doi:https://doi.org/10.1016/j.msec.2016.11.049.

58. Hasan, A.; Soliman, S.; El Hajj, F.; Tseng, Y.T.; Yalcin, H.C.; Marei, H.E. Fabrication and in Vitro Characterization of a Tissue Engineered PCL-PLLA Heart Valve. Sci. Rep. 2018, 8, 1–14, doi:10.1038/s41598-018-26452-y.

59. Wachirahuttapong, S., Thongpin, C., & Sombatsompop, N. (2016). Effect of PCL and Compatibility Contents on the Morphology, Crystallization and Mechanical Properties of PLA/PCL Blends. Energy Procedia, 89, 198–206. doi:10.1016/j.egypro.2016.05.026

60. Lasprilla, A. J. R., Martinez, G. A. R., Lunelli, B. H., Jardini, A. L., & Maciel, R. (2012). Poly-lactic acid synthesis for application in biomedical devices — A review. Biotechnology Advances, 30, 321–328. https://doi.org/10.1016/j.biotechadv.2011.06.019

61. Drumright, R. E., Gruber, P. R., & Henton, D. E. ,2000, polylactid acid techology advance material. 12, 1841-1846.

62. Shadi Hassanajilia, Ali Karami-Poura, Ahmad Oryanb, Tahereh Talaei-Khozanic, 2019, Preparation and characterization of PLA/PCL/HA composite scaffolds using indirect 3D printing for bone tissue engineering, Materials Science & Engineering C 104 (2019) 109960, https://doi.org/10.1016/j.msec.2019.109960

63. Pitjamit, S.; Thunsiri, K.; Nakkiew, W.; Wongwichai, T. The Possibility of Interlocking Nail Fabrication from FFF 3D Printing PLA/PCL/HA Composites Coated by Local Silk Fibroin for Canine Bone Fracture Treatment. Materials (Basel). 2020, 13.

64. Randall M. German and Animesh Bose, 2020, Binder and Polymer Assisted Powder Processing, Publisher: ASM International, Pages: 273, ISBN: 978-1-62708-275-4, Product code: 05929G.

65. Noroozi, N., Schafer, L. L. and Hatzikiriakos, S. G, 2012, Thermorheological properties of poly (ε-caprolactone)/polylactide blends. Polym Eng Sci; p.2348–2359

66. Zhigang Zak Fang, 2010, Sintering of Advanced Materials fundamentals and processes, View series: Woodhead Publishing Series in Metals and Surface Engineering, Woodhead Publishing in material, 1st Edition - September 27, 2010, eBook ISBN: 9781845699949.

67. Callister, W. D., & Rethwisch, D. G. (2018). Materials Science and Engineering An Introduction Tenth Edition (10th Edition)..

68. Arnaldo D. Valino., John Ryan C. Dizon., Alejandro H. Espera Jr., Qiyi Chen., Jamie Messman., Rigoberto C. Advincula., 2019, Advances in 3D Printing of Thermoplastic Polymer Composites and Nanocomposites., Advances in 3D Printing of Thermoplastic Polymer Composites and Nanocomposites, Progress in Polymer Science, doi:https://doi.org/10.1016/j.progpolymsci.2019.101162

69. Aldabib, J.M.; Ishak, Z.A.M, 2020, Effect of Hydroxyapatite Filler Concentration on Mechanical Properties of Poly (Methyl Methacrylate) Denture Base. SN Appl. Sci. 2020, 2, 1–14, doi:10.1007/s42452-020-2546-1.

70. D. Espalin., K. Arcaute., D. Rodriguez Sanz., F. Medina, M. Posner., R. Wicker., 2010, Fused deposition modeling of patient-specific polymethylmethacrylate implants, Rapid Prototyping Journal 16(3)164-173.

71. Dawoud. M., I. Taha, S.J. Ebeid., 2016, Mechanical behaviour of ABS: An experimental study using FDM and injection moulding techniques, Journal of Manufacturing Processes 21 39-45.

72. Doyle, S.E.; Henry, L.; McGennisken, E.; Onofrillo, C.; Di Bella, C.; Duchi, S.; O'connell, C.D.; Pirogova, 2021, E. Characterization of Polycaprolactone Nanohydroxyapatite Composites with Tunable Degradability Suitable for Indirect Printing. Polymers (Basel). 2021, 13, 1–14, doi:10.3390/polym13020295.

73. Fong, M. K., Nasrull, M., Rahman, A., Mubarak, A., & Arifin, T. (2021). Characterization , Thermal and Biological Properties of PCL / PLA / PEG / N-HA Composites. 11(2), 9017–9026.

74. Hapsari, D.N.; Wardani, S.C.; Firdausya, W.A.; Amaturrohman, K.; Wiratama, H.P. The Effect of Addition of Hydroxyapatite from Skipjack Tuna (Katsuwonus Pelamis) Fish Bone Flour to the Transverse, Impact, and Tensile Strength of Heat Cured Acrylic Resin. J. Dentomaxillofacial Sci. 2020, 5, 94, doi:10.15562/jdmfs.v5i2.1016.

75. Haq, R., Haq, A., Taib, I., Nasrull, M., Rahman, A., Haw, F., Abdullah, H., Ahmad, S., Mubarak, A., Ariffin, T., & Hassan, M. F. (2019). Mechanical Properties of PCL / PLA Composite Sample Produced from 3D Printer and Injection Molding. 5, 97–101.

76. Ali, J., Rezaei-tavirani, M., Biazar, E., K, S. H., & Jahandideh, R. (2011). Mechanical Properties of Chitosan-Starch Composite Filled Hydroxyapatite Micro- and Nanopowders. Hindawi Publishing Corporation Journal ofNanomaterials, 2011, 18–23. https://doi.org/10.1155/2011/391596.

77. Imre, B., Pukánszky, B., 2013, Compatibilization in Bio-Based and Biodegradable Polymer Blends. European Polymer Journal, 49, 1215-1233. http://dx.doi.org/10.1016/j.eurpolymj.2013.01.019.

78. Fortelny, I., Ujcic, A., Fambri, L., & Slouf, M. (2019). Phase Structure, Compatibility , and Toughness of PLA / PCL Blends: A Review. 6, 1–13. https://doi.org/10.3389/fmats.2019.00206.

79. Cóta, L. F., Patricia, K., Licona, M., Lunz, N., Ribeiro, A. A., Morejón, L., Oliveira, M. V. De, & Pereira, L. C. (2016). Hydroxyapatite Nanoparticles: Synthesis by Sonochemical Method and Assessment of Processing Parameters via Experimental Design. Materials Science Forum, 869, 896–901. https://doi.org/10.4028/www.scientific.net/MSF.869.896.

80. P.Y.Chena, A.G.Stokesb, J. McKittrick, 2009, Comparison of the structure and mechanical properties of bovine femur bone and antler of the North American elk (Cervus elaphus canadensis), Acta

Biomaterialia, Volume 5, Issue 2, February 2009, Pages 693-706, https://doi.org/10.1016/j.actbio.2008.09.011.

81. Gong, M., Zhao, Q., Dai, L., Li, Y., & Jiang, T. (2017). Journal of Asian Ceramic Societies Fabrication of polylactic acid / hydroxyapatite / graphene oxide composite and their thermal stability , hydrophobic and mechanical properties. Integrative Medicine Research, 5(2), 160–168. https://doi.org/10.1016/j.jascer.2017.04.001.

82. M.S. Singhvi, S.S. Zinjarde, D.V. Gokhale, 2019, Poly-Lactic acid (PLA): synthesis and biomedical applications, Journal of applied microbiology.

83. Liu H, Song W., Chen F, Guo L, Zhang J., 2011, Interaction of microstructure and interfacial adhesion on impact performance of Polylactide (PLA) ternary blends. Macromolecules 2011, 44: 1513-1522.

84. Visco A., Nocita D., Giamporcaro A., Ronca S, Forte G, Pistone A, Espro C., 2017, Effect of ethyl ester L-lysine triisocyanate addition to produce reactive PLA/PCL bio-polyester blends for biomedical applications. Journal of the Mechanical Behavior of Biomedical Materials, 68: 308-317.

85. Molinero-Mourelle, P.; Canals, S.; Gómez-Polo, M.; Sola-Ruiz, M.; Highsmith, J.D.R.; Viñuela, A. Polylactic Acid as a Mate-rial for Three-Dimensional Printing of Provisional Restorations. Int. J. Prosthodont. 2018, 31, 349–350. https://doi.org/10.11607/ijp.5709.

86. Triyono, J., Alfiansyah, R., Sukanto, H., Ariawan, D., & Nugroho, Y. (2020). Fabrication and characterization of porous bone scaffold of bovine hydroxyapatite-glycerin by 3D printing technology. Bioprinting, e00078. doi:10.1016/j.bprint.2020.e00078.

87. Solechan, S.; Suprihanto, A.; Widyanto, S.A.; Triyono, J.; Fitriyana, D.F.; Siregar, J.P.; Cionita, T. Characterization of PLA/PCL/Nano-hydroxyapatite (nHA) Biocomposites Prepared via Cold Isostatic Pressing. Polymers 2023, 15, 559. https://doi.org/10.3390/polym15030559